Post-transcriptional Regulation of α-1-Antichymotrypsin by MicroRNA-137 in Chronic Heart Failure and Mechanical Support

Sjoukje I. Lok, MD; Alain van Mil, PhD; Niels Bovenschen, PhD; Petra van der Weide, BSc; Joyce van Kuik, BSc; Dick van Wichen, BSc; Ton Peeters, BSc; Erica Siera, BSc; Bjorn Winkens, PhD; Joost P.G. Sluijter, PhD; Pieter A. Doevendans, MD, PhD; Paula A. da Costa Martins, PhD; Nicolaas de Jonge, MD, PhD; Roel A. de Weger, PhD

Background—Better understanding of the molecular mechanisms of remodeling has become a major objective of heart failure (HF) research to stop or reverse its progression. Left ventricular assist devices (LVADs) are being used in patients with HF, leading to partial reverse remodeling. In the present study, proteomics identified significant changes in α-1-antichymotrypsin (ACT) levels during LVAD support. Moreover, the potential role of ACT in reverse remodeling was studied in detail.

Methods and Results—Expression of ACT mRNA (quantitative-polymerase chain reaction) decreased significantly in post-LVAD myocardial tissue compared with pre-LVAD tissue (n=15; $P<0.01$). Immunohistochemistry revealed that ACT expression and localization changed during LVAD support. Circulating ACT levels were elevated in HF patients (n=18) as compared with healthy controls (n=6; $P=0.001$) and normalized by 6 months of LVAD support. Because increasing evidence implicates that microRNAs (miRs) are involved in myocardial disease processes, we also investigated whether ACT is post-transcriptionally regulated by miRs. Bioinformatics analysis pointed miR-137 as a potential regulator of ACT. The miR-137 expression is inversely correlated with ACT mRNA in myocardial tissue. Luciferase activity assays confirmed ACT as a direct target for miR-137, and in situ hybridization indicated that ACT and miR-137 were mainly localized in cardiomyocytes and stromal cells.

Conclusions—High ACT plasma levels in HF normalized during LVAD support, which coincides with decreased ACT mRNA in heart tissue, whereas miR-137 levels increased. MiR-137 directly targeted ACT, thereby indicating that ACT and miR-137 play a role in the pathophysiology of HF and reverse remodeling during mechanical support. (***Circ Heart Fail*. 2013;6:853-861.**)

Key Words: ACT ■ heart failure ■ LVAD ■ remodeling ■ serpina-3

Heart failure (HF) is considered a highly complex clinical syndrome, manifested by many cardiac and extracardiac features.[1] The complex sequelae of HF, which take place in the heart, are generally referred to as cardiac remodeling and involve molecular and cellular processes that result in changes of size, shape, and function of the heart after injury or stress stimulation.[1,2] Left ventricular assist devices (LVADs) provide a unique and valuable opportunity to investigate reverse remodeling in humans, because they provide volume and pressure unloading of the left ventricle, thereby reversing the compensatory responses of the overloaded myocardium.[3,4]

Clinical Perspective on p 861

There is substantial interest in applying proteomics to obtain better understanding of disease processes and to develop new biomarkers for diagnosis and early detection of cardiovascular diseases.[5,6] The purpose of the present study was to investigate proteomic changes in reverse remodeling during LVAD support. Because the degree of reverse remodeling is more pronounced in patients with nonischemic dilated cardiomyopathy (DCM),[7] we focused on this subset of patients.

Recently, we found that levels of α-1-antichymotrypsin (ACT) expression decrease in myocardial tissue during pulsatile-LVAD support, which was detected by proteomics and confirmed by immunosorbent assays.[8] However, the molecular pathways regulating ACT expression in the heart were not explored.

Clinically, pulsatile-LVAD support is being replaced by continuous-flow LVAD (cf-LVAD) support. Therefore, we performed proteomics in plasma and heart tissue of DCM

Received July 19, 2012; accepted April 22, 2013.

From the Departments of Cardiology (S.I.L., A.v.M., J.P.G.S., P.A.D., N.d.J.) and Pathology (N.B., P.v.d.W., J.v.K., D.v.W., T.P., E.S., R.A.d.W.), University Medical Center, Utrecht, The Netherlands; Departments of Methodology and Statistics (B.W.) and Cardiology (P.A.d.C.M.), University of Maastricht, Maastricht, The Netherlands; and ICIN Netherlands Heart Institute, Utrecht, The Netherlands (A.v.M., J.P.G.S., P.A.D.).

The online-only Data Supplement is available at http://circheartfailure.ahajournals.org/lookup/suppl/doi:10.1161/CIRCHEARTFAILURE.112.000255/-/DC1.

Correspondence to Sjoukje Irene Lok, MD, University Medical Center Utrecht, Department of Cardiology, Huispostnummer H04.312, Postbus 85500, 3508 GA Utrecht, The Netherlands. E-mail s.lok@umcutrecht.nl

Circ Heart Fail **is available at http://circheartfailure.ahajournals.org** **DOI: 10.1161/CIRCHEARTFAILURE.112.000255**

patients, supported with a cf-LVAD. This approach suggested a potential role of ACT during reverse remodeling in cf-LVAD, which was experimentally confirmed in individual patients by ELISA, quantitative-polymerase chain reaction, and protein localization.

MicroRNAs (miRs) are small, noncoding RNAs that bind mRNAs at their 3′-untranslated regions (UTRs), stimulating mRNA degradation or inhibiting protein translation.[9] Delineating the role of miRs in post-transcriptional gene regulation offers new insight into the mechanisms by which the heart adapts to mechanical support. Moreover, miRs can be important hallmarks for recovery or deterioration and can be used as a therapeutic target in HF.[10] Therefore, the post-transcriptional regulation of ACT by miRs was investigated.

This study revealed a potential role of ACT, and its post-transcriptional regulator miR-137, in the pathophysiology of HF and reverse remodeling during mechanical support.

Methods

Study Population

Eighteen patients were included with a nonischemic DCM supported with a cf-LVAD (Heart-Mate II, Thoratec, CA) as bridge to heart transplantation (HTx). Plasma was collected before and 1, 3, and 6 months after LVAD implantation. Control plasma was collected from 6 healthy individuals.

Of the 18 patients included, 15 underwent HTx. Myocardial tissue of each individual patient was collected at time of LVAD implantation (pre-LVAD) and from the explanted left ventricle (post-LVAD), outside the suture area of the inflow cannula. Control myocardial tissue was obtained from 3 donor hearts declined for HTx (because of noncardiac reasons) and from biopsies of 7 donor hearts during HTx surgery. All LVAD patients gave written informed consent for the use of their tissues for research purposes.

2-Dimensional Difference Gel Electrophoresis

With the use of fluorescent 2-dimensional difference gel electrophoresis (2D-DIGE), a comparative analysis was made of protein expression in tissue and plasma of DCM patients before and after cf-LVAD implantation. Paired premyocardial and postmyocardial tissue of 8 patients and 4 controls were analyzed. In addition, EDTA plasma of 8 DCM patients and 5 controls was used before implantation and 6 months after implantation (online-only Data Supplement). Differentially expressed proteins were excised and identified by tandem mass spectrometry (online-only Data Supplement).

Plasma Levels of ACT

EDTA blood was centrifuged at 3000 rpm for 10 minutes, plasma was collected and stored at −20°C. Circulating ACT was determined by ELISA (online-only Data Supplement).

ACT mRNA and miR-137 Levels

Total RNA was isolated from 20 sections of 10-μm snap-frozen myocardial tissue using miRNeasy Mini Kit (Qiagen Inc, Austin, TX). Copy DNA for ACT was synthesized with superscript III, oligo-dT, and random primers (Life Technologies, Bleiswijk, The Netherlands). mRNA expression of ACT was determined by quantitative-polymerase chain reaction on the LightCycler-480 (Roche Diagnostics BV, Almere, The Netherlands), as described previously.[11] A detailed description is provided in the online-only Data Supplement. For miR-137, a 2-step protocol consisting of reverse transcription with an miR-specific primer followed by quantitative-polymerase chain reaction with a TaqMan probe was performed on the ViiA 7 (Life Technologies).

Immunohistochemistry

The expression of ACT and its major target for proteinase inhibition, cathepsin G (CG), was analyzed by immunohistochemistry in formalin-fixed paraffin-embedded sections. Endogenous peroxidase was blocked with H_2O_2 for 15 minutes. Sections were pretreated with either citrate (ACT) or EDTA (CG) and incubated with primary antibody diluted in PBS/1% BSA for 1 hour. (ACT, diluted 1:50, rabbit anti-human ACT, Dako, Glostrup, Denmark; CG diluted 1:100, mouse anti-human CG, Abcam, Cambridge, MA). Power Vision poly-Anti-Rabbit IgG (Immunovision Technologies, Hillsborough, FL) and RamPo (diluted 1:500+10% NHuS [normal human serum], polyclonal rabbit anti-mouse Immunoglobulin HRP [horseradish peroxidase], Dako) were used as secondary antibodies for ACT and CG, respectively. The slides were developed with DAB (3,3′-diaminobenzidine-hydrochloride) solution for 10 minutes. The nuclei were counterstained with Mayer's Haematoxylin. In every section, 3 areas were selected at random and the ACT staining of cardiomyocytes, epithelial and stromal cells was scored and the modus was calculated. ACT expression was analyzed using a scoring system; 0=no staining, 1=weak, 2=moderate, and 3=strong. This was performed individually by 3 observers, from which the intraobserver agreement was assessed using unweighted and weighted kappas.

Double-staining ACT and Anticardiac Actin

After staining with the primary antibody for ACT (diluted 1:50, rabbit anti-human ACT, Dako), slides were incubated with swine anti-rabbit Ig TRITC (tetramethylrhodamine isothiocyanate)-labeled (Dako, 1:40) in PBS and 10% AB serum. After a wash in PBS/Tween-20, the slides were incubated with a solution of PBS and 10% normal rabbit serum for 30 minutes. After decanting the solution, the slides were horizontally incubated with monoclonal antiactin (α-sarcomeric) antibody produced in mouse (Sigma-Aldrich Inc, St. Louis, CA, 1:500) in PBS and 10% normal rabbit serum. Incubation was followed by a washing step in PBS/Tween-20. The slides were horizontally incubated with rabbit anti-mouse fluorescein isothiocyanate (Dako, 1:50) in PBS and 10% AB-serum. After a wash with PBS/Tween-20, the slides were incubated with Topro-3 iodide (Life Technologies, 1:500) in PBS Tween-20 and coverslips were mounted onto object glasses using vectashield-mounting medium (VectorLaboratories Inc, Burlingame, CA).

In Situ Hybridization for ACT mRNA and miR-137

In situ hybridization (ISH) for ACT mRNA was performed on tissue slides from freshly frozen paired myocardial samples of 4 patients pre- and post-LVAD support and of 2 controls (donor hearts declined for HTx; online-only Data Supplement). Negative (ISH without probe) and positive controls were included. To test the specificity of the ISH signal of ACT, a nonrelevant probe (interleukin-2) was tested in parallel.

Locked nucleic acid (LNA) hybridization probes for miR-137 and negative control miRCURY LNA Sense (scramble) were conjugated with 3′- 5′digoxigenin. Positive control probe U6 was conjugated with 5′digoxigenin. miR in situ was performed as described at http://www.exiqon.com/insitu. All LNA reagents were obtained from Exiqon (Vedbaek, Denmark).

miR Transfection

The human hepatoma cell line (HepG2) was used as a model to examine expression of ACT mRNA after miR-137 transfection. Cells were resuspended in normal growth medium to 1×10^5 cells/500 mL. A total of 0.5 μL of interleukin-6 was added to stimulate ACT production. Pre-miR miRNA Precursor Molecules for miR-137 (PM10513) or a Negative Precursor Control (AM17110; nontargeting sequence) were transfected with 1 μL lipofectamine RNAiMax, according to the instruction of the manufacturer (Life Technologies). In addition, some cells were left untreated (nontransfection). As a positive control for HepG2 transfection, miRNA Precursor molecules for miR-1 (PM10617) were transfected and the effect on protein tyrosine kinase-9, a validated miR-1 target, was determined. After 48 hours, total RNA of the HepG2 cells was isolated as described earlier. The transfection experiments were performed 7× and 10× for miR-1 and mir-137, respectively.

Luciferase Assay

The 3′UTR of ACT was cloned into the pMIR-REPORT Luciferase vector (Life Technologies). Mutations for the miR-137 target site were generated by QuikChange II Site-Directed Mutagenesis (Agilent Technologies, Amstelveen, The Netherlands). To determine the suppression efficiency of miR-137, 4 luciferase experiments were performed. In each experiment 2×10^5 HEK293 (human embryonic kidney 293) cells were cotransfected with 200 ng pMIR-REPORT-ACT-3′UTR Luciferase vector, or the mutated vector and a pMIR-REPORT β-gal control plasmid for normalization of transfection efficiency. In addition, 50 nmol/L precursor miR-137, or a negative control precursor miR, or an miR without predicted target sites for ACT were introduced by using Lipofectamine 2000 (Life Technologies). Luciferase and β-galactosidase activity was assessed after 48 hours with the Luciferase Assay System and β-galactosidase Enzyme Assay System (Promega), respectively, as described before.[12]

Statistical Analysis

Because of the small sample size and expected non-normality, the ACT isoforms and quantitative-polymerase chain reaction data (for ACT and miR-137) were presented as median with first and third quartile (Q1–Q3), and evaluated with the Wilcoxon signed-rank test. Plasma data were plotted and evaluated using the mixed-model analysis with a random intercept to account for the dependency between repeated measurements within the same patient. Data from patients pre- and post-LVAD were compared with those of healthy controls, using Mann–Whitney *U* test. The interobserver variability of ACT expression in the heart was indicated by unweighted and weighted kappas. The statistical analysis of 2D-DIGE gel spot volume quantification, transfection experiments, and the luciferase reporter assays were presented as mean and SEM and evaluated with the paired samples *t* test. A $P\leq0.05$ was considered significant. All analyses were performed using SPSS, version 18 (SPSS, Inc, Chicago, IL).

Results

Patient Characteristics

Patient demographics are shown in the Table. All patients presented initially with HF New York Heart Association class IV despite optimal medical therapy, including intravenous inotropic therapy. Median age was 43 years (Q1–Q3, 28–48), 78% (n=14) was male and 44% (n=8) had a familial cause of DCM. A total of 61% (n=11) of the patients had a cardiac resynchronization therapy defibrillator or implantable cardioverter defibrillator before cf-LVAD implantation. The median duration of mechanical support, based on the patients who already underwent HTx (n=15), was 282 days (Q1–Q3, 207–521).

2D-DIGE Identifies ACT Changes in Plasma and Myocardial Tissue During LVAD Support

2D-DIGE on myocardial tissue of 8 DCM patients identified 40 proteins that changed significantly during cf-LVAD support, of which 9 were upregulated. 2D-DIGE on plasma of 8 DCM patients identified 97 proteins that were significantly different in the pre-pool versus the postpool. Ninety proteins were downregulated and 7 were upregulated. Of all proteins, only ACT changed significantly in both tissue and plasma during cf-LVAD support. Five different isoforms of ACT were detected in myocardial tissue, of which 2 were significantly downregulated during cf-LVAD support (1.78–2.39 downfold; Figure 1A–1F). Four different isoforms of circulating ACT were detected, all of them being significantly downregulated during cf-LVAD (2.03–2.74 downfold; Figure 1G–1J).

Table. Patient Demographics

Characteristic*	Patients (n=18)
Age, y	43.0 (28.0–48.0)
Male, %	14 (78%)
Body mass index, kg/m^2	24.2 (20.1–26.0)
Heart failure duration, d	1675 (416–1954)
Diabetes mellitus, %	0 (0%)
Hypertension, %	1 (6%)
Hyperlipidemia, %	4 (22%)
CVA/TIA, %	5 (28%)
NYHA classification IV, %	18 (100%)
Etiology of nonischemic DCM, %	
Idiopathic	5 (28%)
Familial†	8 (44%)
Myocarditis	2 (11%)
Peripartum	1 (6%)
Toxic (drugs/medication)	2 (11%)
Preoperative intervention (CRTD/ICD), %	11 (61%)
Days of LVAD support‡	282 (207–521)

CRTD indicates cardiac resynchronization therapy defibrillator; CVA, cerebrovascular accident; DCM, dilated cardiomyopathy; ICD, implantable cardioverter defibrillator; LVAD, left ventricular assist device; NYHA, New York Heart Association; and TIA, transient ischemic attack.

*Categorical data are presented as number (%) and continuous data as median (25%–75% percentile).

†Familial DCM is defined if the patient has one or more family members diagnosed with idiopathic DCM or has a first-degree relative with an unexplained sudden death under the age of 35 y.

‡Days of LVAD support are based on the patients who already underwent heart transplantation (n=15).

Elevated Circulating ACT Levels Normalize During Mechanical Support

ACT plasma levels were significantly elevated in end-stage HF patients before LVAD implantation as compared with levels in healthy controls (P=0.001; Figure 2A). After 1 month of LVAD support, the concentration of circulating ACT showed a nonsignificant increase (P=0.08). However, after 3 and 6 months of LVAD support, plasma ACT decreased significantly compared with baseline (both P<0.001) and ultimately reached a similar level as of controls (P=0.18).

ACT mRNA and Protein Expression Change During Mechanical Support

Myocardial mRNA expression of ACT was increased in DCM patients before cf-LVAD implantation in comparison with controls, but did not reach significance (P=0.26; Figure 2B). After cf-LVAD support, mRNA ACT decreased significantly (median change, −0.41, Q1−Q3, −1.71 to −0.17; P=0.004) to levels lower than that of controls (P=0.01).

Localization and distribution of ACT protein in the myocardium during cf-LVAD support was determined by immunohistochemistry. ACT-expression before LVAD support was weak to moderate in the cardiomyocytes, whereas the expression of ACT in the endothelium and stromal cells in the interstitium was strong (arrowheads; Figure 3A). If present,

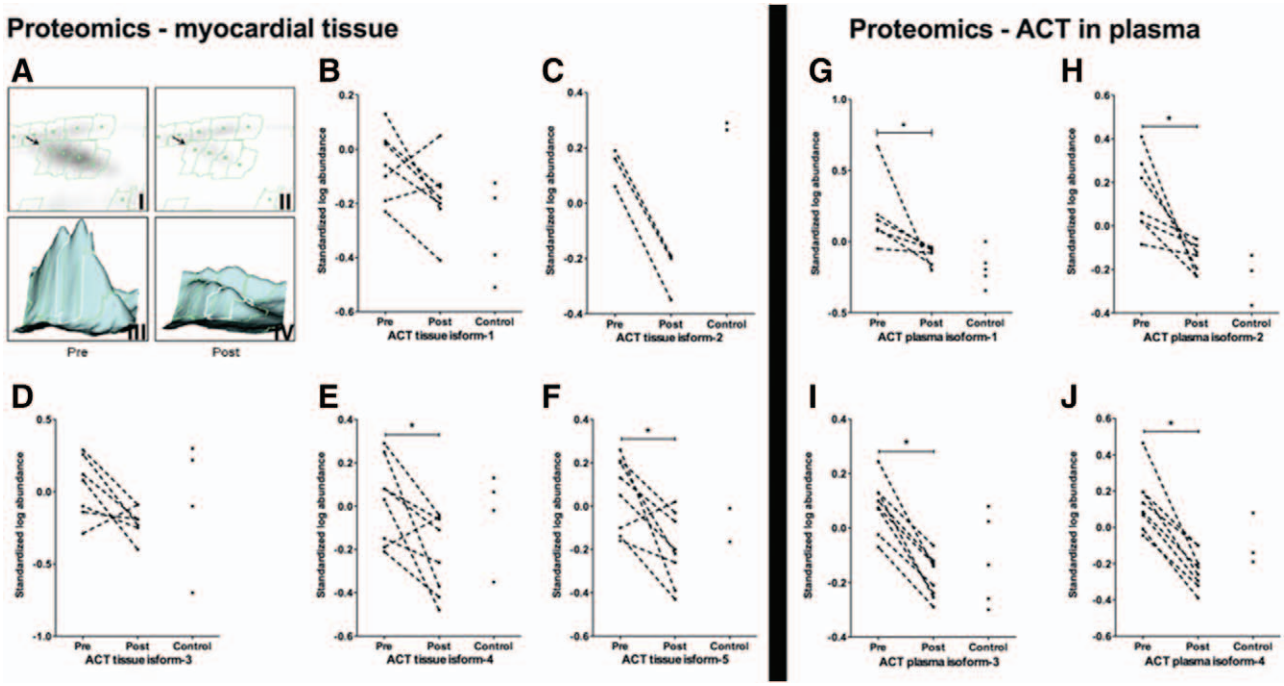

Figure 1. Two-dimensional (2D) difference gel electrophoresis of myocardial tissue (n=8 patients, n=4 controls) and plasma (n=8 patients, n=5 controls) before and after continuous-flow-left ventricular assist device (cf-LVAD) implantation. Representative 2D-image of α-1-antichymotrypsin (ACT) in myocardial tissue pre- and post-LVAD (**A**). Proteomics of myocardial tissue (**B**–**F**) revealed 2 of 5 ACT isoforms that were significantly downregulated in the post-LVAD sample as compared with pre-LVAD (**E**, **P*=0.04; **F**, **P*=0.02). Proteomics revealed 4 different isoforms of circulating ACT that changed pre-LVAD as compared with 6 months after LVAD implantation (**G**–**J**). All isoforms were significantly downregulated (**G**, **P*=0.04; **H**, **P*=0.02; **I**, **P*=0.01; **J**, **P*=0.008). Each line represents 1 patient.

inflammatory cells tended to stain as well. After LVAD support (Figure 3B), ACT expression in the cardiomyocytes changed from a diffuse pattern toward an alternating pattern demonstrating either low or strong expression of ACT (on–off effect) in different cardiomyocytes, mainly in the central area of the myocardium. In contrast, expression in the endothelium and in the stromal cells became very low (arrowheads; Figure 3B). In controls (Figure 3C), cardiomyocytes stained weak with only very occasionally an on–off effect. Stromal cells and capillaries stained moderately. The unweighted kappas showed excellent agreement in ACT staining of cardiomyocytes, endothelial tissue, and stromal cells (0.90, 0.85, 0.91, respectively). Moreover, the weighted kappas (linear and quadratic) were even higher (0.91 and 0.92 for cardiomyocytes, 0.87 and 0.89 for endothelial tissue, and both 0.91 for stromal cells).

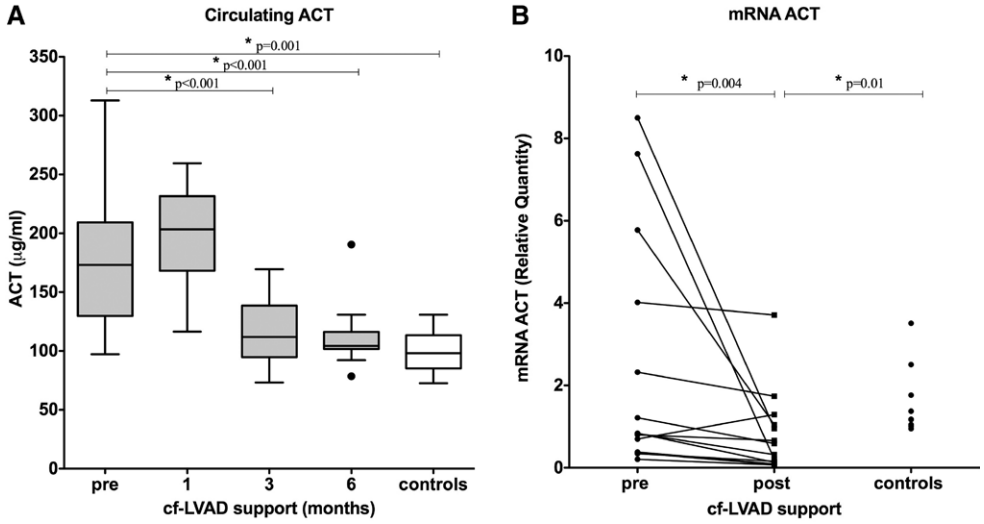

Figure 2. Circulating α-1-antichymotrypsin (ACT) protein and ACT mRNA expression. Circulating ACT (µg/mL) in patients with dilated cardiomyopathy (n=18 patients, n=6 controls) before, and 1, 3, and 6 months after continuous-flow-left ventricular assist device (cf-LVAD) implantation, demonstrated in Tukey boxplots (**A**). After 1 month, there was a nonsignificant increase followed by normalization after 6 months of support. mRNA expression of ACT (**B**). After cf-LVAD support, there was a significant decrease in mRNA to levels lower than that of controls (n=15 patients, n=9 controls). Some interindividual variation was observed.

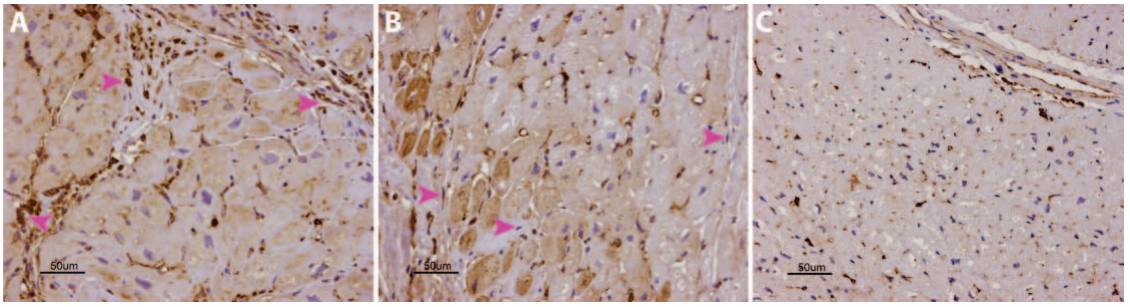

Figure 3. Immunohistochemistry of α-1-antichymotrypsin (ACT) before and after continuous-flow-left ventricular assist device (cf-LVAD) support. Myocardial tissue pre-LVAD (**A**), post-LVAD (**B**) support and control (donor hearts declined for heart transplantation; **C**) was stained. Notice the difference in ACT staining in the cardiomyocytes (diffuse versus on–off effect) and in the stromal cells (pink arrowheads; strong versus no/weak staining) between pre- and post-LVAD tissue. Control tissue showed diffuse cardiomyocyte staining and weak stromal cell staining.

To investigate if the on–off effect was caused by induced cell death, we performed double immunohistochemistry staining with anticardiac actin and ACT. Merging the images clearly showed that the contractile elements were present both in the ACT stained and in the nonstained cells (Figure 4A–4D), indicating that apoptosis is not related to ACT expression. CG expression was not localized in cardiomyocytes, endothelium, capillaries, or extracellular matrix, but was only present in few scattered mast cells (data not shown).

Post-transcriptional Regulation of ACT by miR-137

According to two major miR target prediction databases, miRanda[13] and Targetscan,[14] ACT is a potential target gene of miR-137. Interestingly, the measuring of miR-137 levels during cf-LVAD support showed that its expression significantly increased in the myocardial tissue (P=0.01; Figure 5).

Whereas in pre-LVAD samples, ACT mRNA was present in cardiomyocytes and stromal cells (Figure 6A), in post-LVAD samples it could only be detected in cardiomyocytes (partly in the nuclei; Figure 6B) and no on–off effect was seen. Furthermore, healthy controls (Figure 6C) revealed low expression of ACT mRNA and only in the cardiomyocytes (mainly in the nuclei). ACT mRNA was widely expressed in placental positive control tissue (Figure 6D). In the parallel experiment demonstrating the specificity of the ACT-probe, interleukin-2 was only expressed in a few interstitial stromal cells (Figure I in the online-only Data Supplement). Curiously, in pre-LVAD samples (Figure 7A and 7B), miR-137 was moderately expressed in cardiomyocytes whereas post-LVAD, miR-137 was expressed in cardiomyocytes and stromal cells (Figure 7C and 7D). A scrambled miR was used as a negative control, showing only a weak background staining (Figure 7E). U6 was used as a positive control, clearly staining the nuclei as expected (Figure 7F).

To address the effect of miR-137 expression on ACT mRNA, we transfected HepG2 cells with miR-137 precursor molecules. Transfection of miR-137 resulted in >50% reduction of ACT mRNA levels (Figure 8A), compared with non-transfected cells (P<0.001; mean 45.4±7.6 SEM). As a positive control for transfection, delivery of miR-1 gave rise to significantly lesser mRNA of its validated target protein tyrosine kinase-9 in comparison to the nontransfected cells (P=0.001,

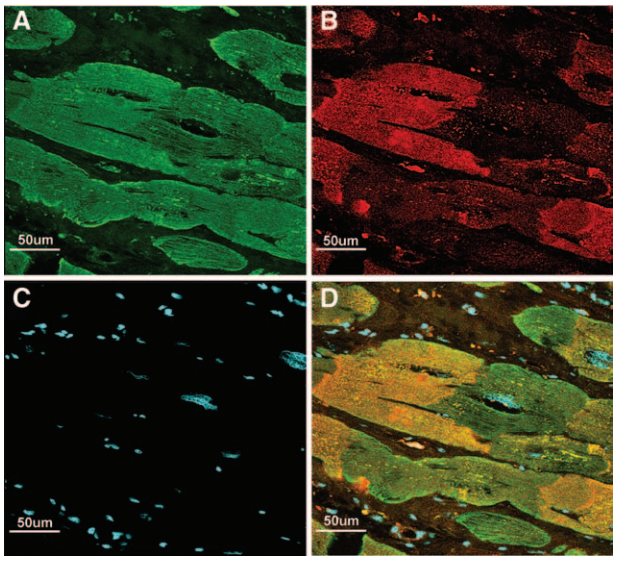

Figure 4. Fluorescence double staining of α-1-antichymotrypsin (ACT) and anticardiac actin. Fluorescence immunohistochemistry of myocardial tissue of a patient with dilated cardiomyopathy after continuous-flow-left ventricular assist device support. Anti-cardiac actin (green; **A**), ACT (red; **B**), nuclei of cardiomyocytes (blue; **C**), and merged image (**D**). This indicated that anticardiac actin is present both in the cells positive and negative for ACT.

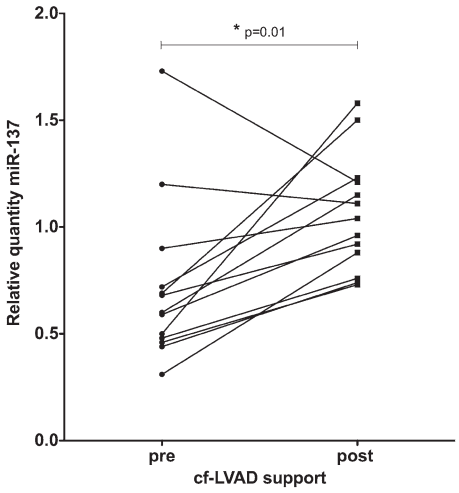

Figure 5. Relative quantification of microRNA (miR)-137 during continuous-flow-left ventricular assist device (cf-LVAD) support. The expression of miR-137 was significantly upregulated post-LVAD (n=13).

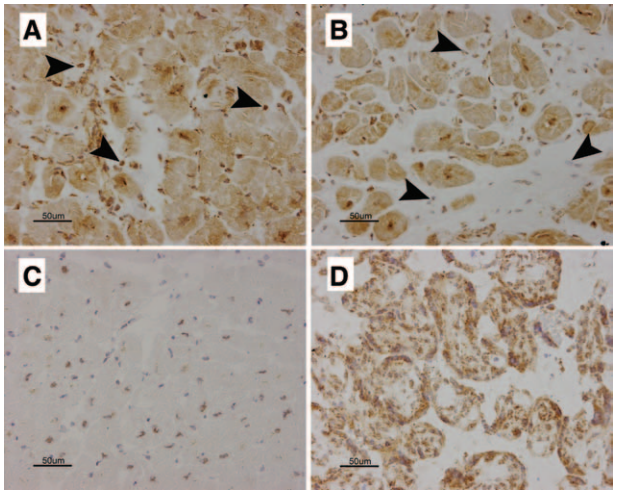

Figure 6. In situ hybridization of α-1-antichymotrypsin (ACT). mRNA of ACT in pre-left ventricular assist device (LVAD) samples was mainly located in the cardiomyocytes and stromal cells (arrowheads; **A**). Post-LVAD mRNA of ACT was only visible in cardiomyocytes, stromal cells stained very weak (arrowheads; **B**). In healthy controls, mRNA of ACT was mainly expressed in the nuclei and weakly in the cardiomyocytes (**C**). Placental tissue stained positive for mRNA of ACT (**D**).

with outlier *P*=0.28; Figure 8B). Mean mRNA expression of protein tyrosine kinase-9 in the HepG2 cells after transfection of miR-1 was 34.4±9.7 SEM (without outlier) and 63.6±30.3 SEM (with outlier).

To further confirm the functionality of the miR-137 target site in ACT, we cloned the ACT 3′UTR into a luciferase reporter vector. Firefly luciferase was placed under post-translational control of the native 3′UTR of ACT or an ACT 3′UTR harboring a mutated miR-137 target site. Cotransfection of synthetic miR-137 decreased ACT 3′UTR reporter activity (miR-137 versus nontargeting miR, *P*=0.006; miR-137 versus no miR, *P*=0.002), whereas no sensitivity was observed after cotransfection of a control, nontargeting miR (Figure 8C). In contrast, an ACT 3′UTR reporter with a mutated miR-137 target site showed no sensitivity to miR-137 transfection (Figure 8D). Together, these data indicate the presence of a functional miR-137 target site in the 3′UTR of ACT, confirming ACT as a direct target gene of miR-137.

Discussion

In the present study, it is shown that ACT levels decrease both in heart tissue and in plasma samples of cf-LVAD supported HF patients, suggesting a possible role for ACT in reverse remodeling. Immunohistochemically, a homogenous expression pattern of ACT within each individual cardiomyocyte was observed post-LVAD, whereas the expression levels of ACT between cardiomyocytes varied. This alternated expression was not because of apoptosis. The ACT staining in stromal cells in between the cardiomyocytes showed a strong decrease after LVAD support, both at protein (immunohistochemistry) and mRNA (ISH) levels, and could therefore be the main source of the changes observed in plasma ACT during LVAD support. Also, the regulatory function of miRs on ACT was studied. According to miR target prediction databases, only miR-137 was predicted to target ACT. We have shown that by transfecting HepG2 cells with miR-137, mRNA of ACT was decreased >50%, and by using luciferase reporter analysis, including target-site mutagenesis that ACT is a direct target of miR-137. miR-137 was upregulated after cf-LVAD support, which correlates with the reduced mRNA and protein levels of its target ACT. ISH showed that miR-137 expression was mainly localized in the cardiomyocytes as well in stromal cells (post-LVAD), as were ACT mRNA and protein. Of note, ISH is quantitatively not reliable and therefore levels of miR-137 should be interpreted with caution. Unfortunately, it is not possible to analyze the post-transcriptional role of miR-137 on ACT in a murine HF model, because miR-137 will not bind to the UTR of murine ACT mRNA. ISH ACT showed a more homogeneous staining than miR-137 expression, which may imply that regulation of ACT is not strictly regulated, but that regulation of gene transcription is also involved in controlling ACT expression levels.

The role of ACT in HF is unknown. Inflammatory activity is thought to be a key player in the progression of HF. ACT, SERPINA3 (serpin peptidase inhibitor, clade A, member 3), is an acute-phase protein and induces the proinflammatory cytokine tumor necrosis factor-α, and nuclear factor-κB.[15] Interestingly, tumor necrosis factor-α also controls the synthesis of ACT.[16] tumor necrosis factor-α, which is under the control of nuclear factor nuclear factor-κB activation, is produced

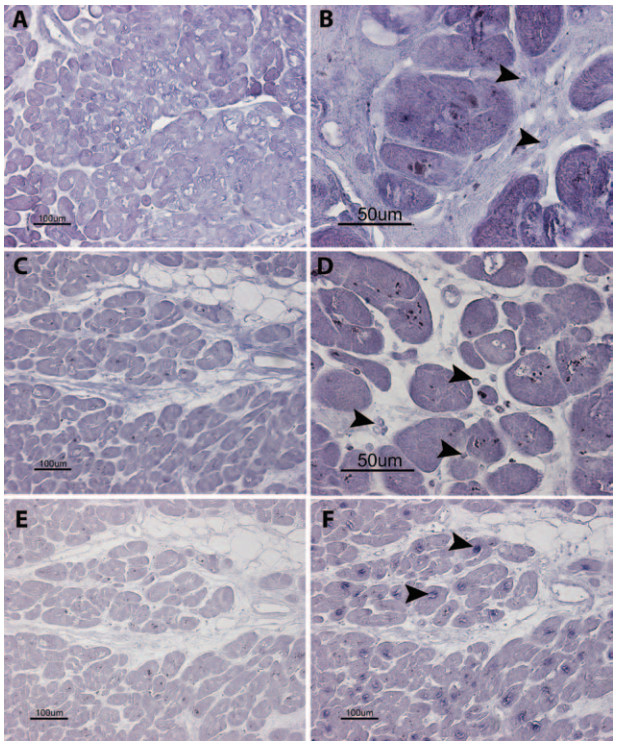

Figure 7. In situ hybridization of microRNA (miR)-137, scramble and U6. In the pre-left ventricular assist device (LVAD) situation (**A** and **B**), miR-137 expression was weak in cardiomyocytes and almost negative in stromal cells (arrowheads) at ×20 (**A**) and at ×40 magnification (**B**). Post-LVAD (**C** and **D**), miR-137 staining was positive in stromal cells (arrowheads) and in the cardiomyocytes at ×20 (**C**) and ×40 magnification (**D**). No clear on–off effect was observed. In the negative scramble in situ hybridization (**E**), a weak background staining was observed in the cardiomyocytes (not in the stromal cells). A strong staining of U6 in the nuclei was detected (arrowheads; **F**).

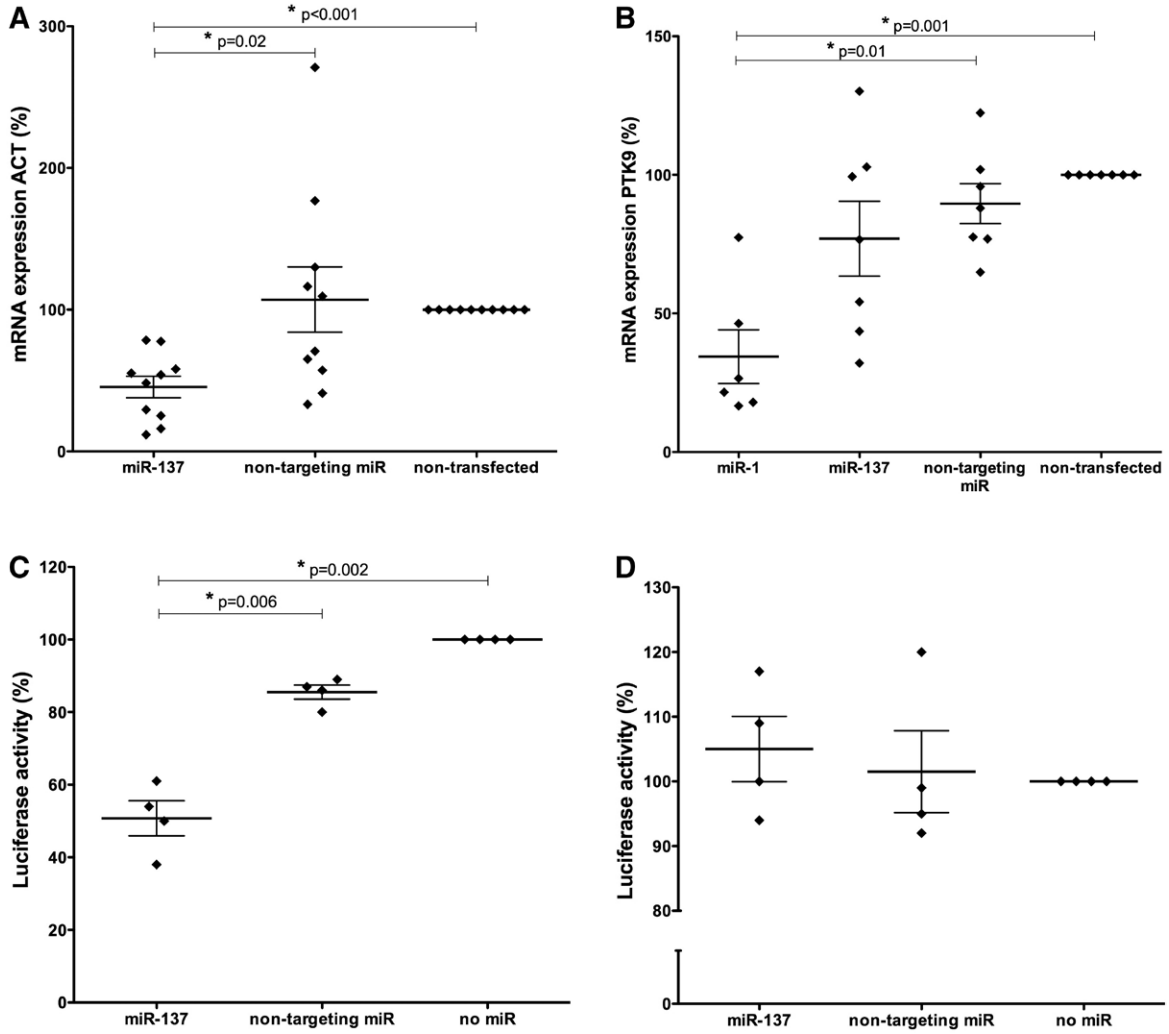

Figure 8. MicroRNA (miR)-transfection and luciferase reporter assay. α-1-antichymotrypsin (ACT) mRNA (**A**) and protein tyrosine kinase-9 (PTK-9) mRNA (**B**) were significantly downregulated after miR-137 (n=10 experiments) and miR-1 transfection (n=7 experiments), in comparison with the nontransfected cells (*P<0.05). The nontransfected human hepatoma cell lines were set on 100%. There was one outlier in the miR-1 transfection PTK-9 experiment; data are presented without this outlier. In the luciferase reporter assays (n=4 experiments; **C** and **D**), luciferase activity was significantly decreased after miR-137 transfection (*P<0.05), in comparison to the nontargeting miR or without miR (**C**). The reduction in luciferase activity was completely abrogated after mutating the predicted miR-137 binding site in ACT 3′untranslated region (**D**). Data are presented in scatter plots as mean and SEM.

locally in the context of HF and has been shown to induce cardiomyocyte apoptosis[17] as well as hypertrophic growth[18] and cardiac remodeling. The initial increase in circulating ACT, which we have demonstrated in the present study, might be caused by the surgical procedure of the cf-LVAD implantation.

ACT is the major inhibitor of the extracellular serine protease activity of CG. Activated neutrophils, macrophages, and mast cells secrete CG into the extracellular space to modulate the immune response.[19,20] The physiological balance between CG and ACT is required for the maintenance of the connective tissue integrity of the heart. Imbalance in favor of CG results in degradation of connective tissue proteins in heart tissue[21] with subsequent cardiomyocyte detachment and apoptosis.[22] A second pathway in which CG can contribute to HF is by converting angiotensin I in angiotensin II, thereby activating the transforming growth factor pathway that results in cardiomyocyte necrosis, hypertrophy, and increased fibrosis.[23] Interestingly, ACT expression was present in several microarray analyses of the failing myocardium.[24–27] These data implicate that ACT limits the proteolytic activity in the human heart by inhibition of CG. LVAD implantation leads to a reversal of HF and accordingly, less inflammation and less mast cells and, thereby, less secretion of CG resulting in less need for ACT. This may explain the decrease in ACT during cf-LVAD support in the present study.

ACT has also been associated with the prevention of skeletal muscle degeneration and injury. Circulating ACT increased early after exercise-induced muscle loss[28] and has been related to the preservation of muscle mass in elderly patients.[29] An increased accumulation of ACT has been demonstrated in muscle fibers of patients with inclusion-body myositis, which is an inflammatory muscle disease characterized by progressive muscle weakness and wasting.[30] ACT is also thought to be protective during ischemia reperfusion by inhibiting neutrophil accumulation into the ischemic-reperfused myocardium and by inactivating cytotoxic metabolites released from neutrophils.[31]

Likewise, ACT was elevated during the first days after an acute coronary syndrome,[32,33] and a persistent postoperative increase was noticed after coronary artery bypass grafting.[34]

Apart from this important role of ACT as a modulator between inflammation and progression of HF by extracellular mechanisms, it may also have important intracellular effects. ACT has the unique ability among serpins to bind to DNA, a property that is independent of its serine protease inhibitory activity.[35] In the present study, mRNA and protein expression of ACT suggest that high amounts of ACT are present within myocardial cells (especially cardiomyocytes and stromal cells) of end-stage HF patients. Moreover, the peculiar staining pattern of ACT in cardiomyocytes, which alters during cf-LVAD support, could indicate an intracellular role for ACT. These intracellular aspects of ACT require further investigation to understand its role in HF.

The clinical experience with LVADs has been valuable for the identification of mechanisms of reverse remodeling because myocardial tissue of patients with end-stage HF can be obtained at the time of implantation and at the time of HTx, after a period of unloading. There are, however, some recognized limitations of molecular studies in LVAD patients. Our study size was small, and the clinical presentation and duration of support are uncontrolled variables, creating a heterogeneous patient population. Furthermore, the present study comprised relatively young patients with a nonischemic origin of systolic HF. To generalize our findings, it is important to confirm and extend the results in other HF populations. It remains to be determined whether ACT can also be an aid in clinical decision making in the management of individual patients. In addition, we tried to confirm our data in murine models. However, the ACT target site for miR137 in humans is not present in mice.

In summary, plasma ACT is elevated in end-stage HF patients and normalizes during mechanical support. ACT expression is directly regulated by miR-137. ACT and miR-137 are mainly localized in the stromal cells and cardiomyocytes during LVAD support. To the best of our knowledge, miR-137 has not been implicated in cardiovascular disease and this is the first study to show its expression in the human heart, and the shift in expression pattern after unloading the heart by cf-LVAD. Because the expression of ACT is directly regulated by miR-137, and their expression levels are inversely related in vivo, it is tempting to speculate that miR-137 and ACT can play an important role in the pathophysiology of HF and either one could possibly serve as a therapeutic target.

Acknowledgments

We sincerely express our appreciation to Fay M.A. Nous, Ankie J.P. van Geffen, Razi Quadir, and Lucien Beckers for their contribution to the laboratory assessments.

Sources of Funding

This work was supported by The Netherlands Heart Foundation (2003B07304 to P.A.D.); the Besluit Subsidies Investeringen Kennisinfrastructuur “Dutch Program for Tissue Engineering” (6746 to P.A.D.). This research forms part of the Project P1.05 LUST (J.P.G.S.) of the research program of the BioMedical Materials institute, cofunded by the Dutch Ministry of Economic Affairs, Agriculture and Innovation.

Disclosures

None.

References

1. Jessup M, Brozena S. Heart failure. *N Engl J Med*. 2003;348:2007–2018.
2. Cohn JN. Structural basis for heart failure. Ventricular remodeling and its pharmacological inhibition. *Circulation*. 1995;91:2504–2507.
3. de Jonge N, van Wichen DF, Schipper ME, Lahpor JR, Gmelig-Meyling FH, Robles de Medina EO, de Weger RA. Left ventricular assist device in end-stage heart failure: persistence of structural myocyte damage after unloading. An immunohistochemical analysis of the contractile myofilaments. *J Am Coll Cardiol*. 2002;39:963–969.
4. Bruggink AH, van Oosterhout MF, de Jonge N, Ivangh B, van Kuik J, Voorbij RH, Cleutjens JP, Gmelig-Meyling FH, de Weger RA. Reverse remodeling of the myocardial extracellular matrix after prolonged left ventricular assist device support follows a biphasic pattern. *J Heart Lung Transplant*. 2006;25:1091–1098.
5. Phizicky E, Bastiaens PI, Zhu H, Snyder M, Fields S. Protein analysis on a proteomic scale. *Nature*. 2003;422:208–215.
6. Hanash S. Disease proteomics. *Nature*. 2003;422:226–232.
7. Guglin M, Miller L. Myocardial recovery with left ventricular assist devices. *Curr Treat Options Cardiovasc Med*. 2012;14:370–383.
8. de Weger RA, Schipper ME, Siera-de Koning E, van der Weide P, van Oosterhout MF, Quadir R, Steenbergen-Nakken H, Lahpor JR, de Jonge N, Bovenschen N. Proteomic profiling of the human failing heart after left ventricular assist device support. *J Heart Lung Transplant*. 2011;30:497–506.
9. Bartel DP. MicroRNAs: genomics, biogenesis, mechanism, and function. *Cell*. 2004;116:281–297.
10. da Costa Martins PA, Salic K, Gladka MM, Armand AS, Leptidis S, el Azzouzi H, Hansen A, Coenen-de Roo CJ, Bierhuizen MF, van der Nagel R, van Kuik J, de Weger R, de Bruin A, Condorelli G, Arbones ML, Eschenhagen T, De Windt LJ. MicroRNA-199b targets the nuclear kinase Dyrk1a in an auto-amplification loop promoting calcineurin/NFAT signalling. *Nat Cell Biol*. 2010;12:1220–1227.
11. Lok SI, Winkens B, Goldschmeding R, van Geffen AJ, Nous FM, van Kuik J, van der Weide P, Klöpping C, Kirkels JH, Lahpor JR, Doevendans PA, de Jonge N, de Weger RA. Circulating growth differentiation factor-15 correlates with myocardial fibrosis in patients with non-ischaemic dilated cardiomyopathy and decreases rapidly after left ventricular assist device support. *Eur J Heart Fail*. 2012;14:1249–1256.
12. van Mil A, Grundmann S, Goumans MJ, Lei Z, Oerlemans MI, Jaksani S, Doevendans PA, Sluijter JP. MicroRNA-214 inhibits angiogenesis by targeting Quaking and reducing angiogenic growth factor release. *Cardiovasc Res*. 2012;93:655–665.
13. Betel D, Wilson M, Gabow A, Marks DS, Sander C. The microRNA.org resource: targets and expression. *Nucleic Acids Res*. 2008;36:D149–D153.
14. Friedman RC, Farh KK, Burge CB, Bartel DP. Most mammalian mRNAs are conserved targets of microRNAs. *Genome Res*. 2009;19:92–105.
15. Braghin E, Galimberti D, Scarpini E, Bresolin N, Baron P. Alpha1-antichymotrypsin induces TNF-alpha production and NF-kappaB activation in the murine N9 microglial cell line. *Neurosci Lett*. 2009;467:40–42.
16. Palomer X, Alvarez-Guardia D, Rodríguez-Calvo R, Coll T, Laguna JC, Davidson MM, Chan TO, Feldman AM, Vázquez-Carrera M. TNF-alpha reduces PGC-1alpha expression through NF-kappaB and p38 MAPK leading to increased glucose oxidation in a human cardiac cell model. *Cardiovasc Res*. 2009;81:703–712.
17. Krown KA, Page MT, Nguyen C, Zechner D, Gutierrez V, Comstock KL, Glembotski CC, Quintana PJ, Sabbadini RA. Tumor necrosis factor alpha-induced apoptosis in cardiac myocytes. Involvement of the sphingolipid signaling cascade in cardiac cell death. *J Clin Invest*. 1996;98:2854–2865.
18. Yokoyama T, Nakano M, Bednarczyk JL, McIntyre BW, Entman M, Mann DL. Tumor necrosis factor-alpha provokes a hypertrophic growth response in adult cardiac myocytes. *Circulation*. 1997;95:1247–1252.
19. Shapiro SD, Campbell EJ, Senior RM, Welgus HG. Proteinases secreted by human mononuclear phagocytes. *J Rheumatol Suppl*. 1991;27:95–98.
20. Pham CT. Neutrophil serine proteases: specific regulators of inflammation. *Nat Rev Immunol*. 2006;6:541–550.
21. Heutinck KM, ten Berge IJ, Hack CE, Hamann J, Rowshani AT. Serine proteases of the human immune system in health and disease. *Mol Immunol*. 2010;47:1943–1955.
22. Sabri A, Alcott SG, Elouardighi H, Pak E, Derian C, Andrade-Gordon P, Kinnally K, Steinberg SF. Neutrophil cathepsin G promotes

detachment-induced cardiomyocyte apoptosis via a protease-activated receptor-independent mechanism. *J Biol Chem*. 2003;278:23944–23954.
23. Jahanyar J, Youker KA, Loebe M, Assad-Kottner C, Koerner MM, Torre-Amione G, Noon GP. Mast cell-derived cathepsin g: a possible role in the adverse remodeling of the failing human heart. *J Surg Res*. 2007;140:199–203.
24. Yang J, Moravec CS, Sussman MA, DiPaola NR, Fu D, Hawthorn L, Mitchell CA, Young JB, Francis GS, McCarthy PM, Bond M. Decreased SLIM1 expression and increased gelsolin expression in failing human hearts measured by high-density oligonucleotide arrays. *Circulation*. 2000;102:3046–3052.
25. Tan FL, Moravec CS, Li J, Apperson-Hansen C, McCarthy PM, Young JB, Bond M. The gene expression fingerprint of human heart failure. *Proc Natl Acad Sci U S A*. 2002;99:11387–11392.
26. Colak D, Kaya N, Al-Zahrani J, Al Bakheet A, Muiya P, Andres E, Quackenbush J, Dzimiri N. Left ventricular global transcriptional profiling in human end-stage dilated cardiomyopathy. *Genomics*. 2009;94:20–31.
27. Seguchi O, Takashima S, Yamazaki S, Asakura M, Asano Y, Shintani Y, Wakeno M, Minamino T, Kondo H, Furukawa H, Nakamaru K, Naito A, Takahashi T, Ohtsuka T, Kawakami K, Isomura T, Kitamura S, Tomoike H, Mochizuki N, Kitakaze M. A cardiac myosin light chain kinase regulates sarcomere assembly in the vertebrate heart. *J Clin Invest*. 2007;117:2812–2824.
28. Sietsema KE, Meng F, Yates NA, Hendrickson RC, Liaw A, Song Q, Brass EP, Ulrich RG. Potential biomarkers of muscle injury after eccentric exercise. *Biomarkers*. 2010;15:249–258.
29. Schaap LA, Pluijm SM, Deeg DJ, Visser M. Inflammatory markers and loss of muscle mass (sarcopenia) and strength. *Am J Med*. 2006;119:526.e9–526.17.
30. Bilak M, Askanas V, Engel WK. Strong immunoreactivity of alpha 1-antichymotrypsin co-localizes with beta-amyloid protein and ubiquitin in vacuolated muscle fibers of inclusion-body myositis. *Acta Neuropathol*. 1993;85:378–382.
31. Murohara T, Guo JP, Lefer AM. Cardioprotection by a novel recombinant serine protease inhibitor in myocardial ischemia and reperfusion injury. *J Pharmacol Exp Ther*. 1995;274:1246–1253.
32. Kaźmierczak M, Sobieska M, Wiktorowicz K, Wysocki H. Changes of acute phase proteins glycosylation profile as a possible prognostic marker in myocardial infarction. *Int J Cardiol*. 1995;49:201–207.
33. Kopetz VA, Penno MA, Hoffmann P, Wilson DP, Beltrame JF. Potential mechanisms of the acute coronary syndrome presentation in patients with the coronary slow flow phenomenon - insight from a plasma proteomic approach. *Int J Cardiol*. 2012;156:84–91.
34. Banfi C, Parolari A, Brioschi M, Barcella S, Loardi C, Centenaro C, Alamanni F, Mussoni L, Tremoli E. Proteomic analysis of plasma from patients undergoing coronary artery bypass grafting reveals a protease/antiprotease imbalance in favor of the serpin alpha1-antichymotrypsin. *J Proteome Res*. 2010;9:2347–2357.
35. Naidoo N, Cooperman BS, Wang ZM, Liu XZ, Rubin H. Identification of lysines within alpha 1-antichymotrypsin important for DNA binding. An unusual combination of DNA-binding elements. *J Biol Chem*. 1995;270:14548–14555.

CLINICAL PERSPECTIVE

Support of the failing heart by a left ventricular assist device has become an important option in the treatment of heart failure. During left ventricular assist device support, signs and symptoms of heart failure stabilize or diminish, and reverse remodeling of the left ventricle may be observed. Mechanisms contributing to the reverse remodeling process are of great interest. The present study showed that plasma levels of α-1-antichymotrypsin are elevated in end-stage heart failure patients as compared with healthy controls and is inversely related to levels of the microRNA-137. α-1-Antichymotrypsin, an acute phase protein, is a major inhibitor of cathpesin G, the latter being associated with degradation of connective tissue integrity and activation of transforming growth factor-pathway. α-1-Antichymotrypsin can also bind to DNA, suggesting it may also have an intracellular effect. These data suggest that α-1-Antichymotrypsin, and its regulator microRNA-137, play a role in the pathophysiology of heart failure and reverse remodeling during mechanical support.